

Measurement of Differential Thick Target Neutron Yields for (p,n) and (d,n) Reactions in Ten's of MeV Region

M. Baba, T. Aoki, S. Yonai*, N. Kawata, M. Hagiwara, T. Miura,
A. Yamadera, T. Nakamura*

Cyclotron and Radioisotope Center, Tohoku University

**Graduate School of Engineering, Tohoku University*

Sendai 980-8578, Japan

babam@cyric.tohoku.ac.jp

ABSTRACT

We have measured energy-angular differential thick target neutron yields (TTY) for C, Al, Ta, W(p,n) reactions at 50 MeV, and Li, Be (d,n) reactions for 25 MeV deuterons with the TOF method using Tohoku University K=110 MeV cyclotron equipped with a beam swinger system and a well collimated TOF line. Neutron spectrum data have been obtained down to ~ 0.8 MeV from the highest energy at several laboratory angles from 0-deg to 90-deg. The results are compared with other experiments and a recent data library LA-150.

Keywords: *neutrons, thick targets, (p,n), (d,n) reactions*

I. INTRODUCTION

Recent progress in accelerator utilization introduces the requirement of various basic data for safe and efficient utilization of accelerator systems^{1), 2)}. Among them, energy-angular differential thick-target neutron yields (TTY) for energetic ions are the fundamental nuclear data which are indispensable for the design of accelerator shielding and accelerator-based neutron sources. For these design works, in particular for the optimization of neutron production targets, neutron emission spectrum should be known accurately over the entire range of secondary energy. However, the data status is very poor both in quantity and quality as shown by a lack of data and serious disagreement among experiments and calculations. In addition, in most of the past experimental data, the measured energy range is limited only in the high energy region.

We are conducting a series of measurements of TTY at Cyclotron and Radioisotope Center, Tohoku University (CYRIC)³⁾ with the time-of-flight technique using a K=110 MeV AVF cyclotron and the beam-swing system⁴⁾. The beam swinger system changes the beam direction to the target and enables to measure angular distributions with a fixed neutron detector setup. This leads to high quality experimental data with high resolution and good signal to noise ratio.

In this paper, we report measurements on C, Al, Ta, W(p,n) reactions at 50 MeV and Li, Be(d,n) reaction at 25 MeV. Carbon is useful for a beam dump and stopper because of low yields and energy of secondary neutrons due to deep negative Q-value of the $^{12}\text{C}(p,n)$ reaction (-18.1 MeV). Aluminum is also a candidate of accelerator beam-lines due to low activation property. Tantalum and tungsten are used for neutron production targets in accelerator-based moderated neutron sources owing to large yields of low energy evaporation neutrons. These features favor moderated neutron sources for the neutron capture therapy (NCT) and neutron analysis. The Li(d,n) reaction is considered as the intense neutron source for International Fusion Materials Irradiation Facility (IFMIF) and the Be(d,n) reaction as the neutron source in therapy and radiography and so on.

In the present experiment, care was taken to obtain the data over the whole range of neutron spectrum to clarify the spectrum shape which is essential for accelerator shielding and targets design. The results are compared with other experimental data available, and the LA-150 data library for (p,n) data.

II. EXPERIMENTAL

II.1 A facility of CYRIC

The layout of the AVF cyclotron in CYRIC is shown in Fig.1^{3),4)}. The cyclotron accelerates protons up to 90 MeV and deuterons up to 65 MeV, and other heavier particles too³⁾. Protons or deuterons accelerated by the AVF cyclotron are transported to the 5th target room (No.5; TR5) which is equipped with a beam swinger system. The beam-swinger system consists of three bending magnets and changes the incident angle of the beam onto the target from -5 deg. to 110 -deg. Using the system, therefore, we can measure the angular distribution of secondary neutrons without changing the detector setup. Besides, TR5 is connected to a 44-m-long well-shielded flight path in which measurements can be done with low-backgrounds and a flight path long enough for determination of the neutron energy by the TOF method. The beam which has transmitted the target is bent by a dipole magnet into a beam dump (carbon) and it enables measurements even for the 0 -deg without interference of background neutrons produced in the beam dump. The beam dump was shielded by shadow-bars of iron and copper from the experimental area.

The beam transported to the target can be chopped to lower the beam frequency to around $1/8$ – $1/9$ with a sinusoidal chopper located between the cyclotron and TR5.

II.2 Target chamber and targets

The targets were setup in a target holder within the vacuum chamber which is centered in the rotation axis of the swinger magnet. Four targets are mounted on the target holder together with a beam-viewer of aluminum-oxide or zinc-sulfide, and moved remotely from the counting room. The targets were 20 mm in diameter to be sufficiently larger than the beam spot (a few to several mm in diameter) to avoid background neutrons from the beam hitting of the holder materials.

The thickness of the target was 15 mm (C), 10 mm (Al), 4.0 mm (Ta), 7.5 mm (Li) and 3.0 mm (Be) to be full-stop thickness for 50 MeV protons (except for Al). The lithium target was a plate of metallic lithium and was fabricated by rolling within an Ar-filled draft chamber to avoid oxidation. The target holder (aluminum) was insulated from the ground and served as a Faraday cup. The targets holder was surrounded with a copper mesh biased to -500 V to suppress secondary electrons from the targets.

The target chamber and the beam dump were shielded by a 1.5 m thick concrete wall with an iron collimator from the detector to reduce neutron and γ -ray backgrounds.

II.3 Data acquisition and running condition

Neutrons emitted from the targets were detected with NE213 scintillation detectors equipped with a pulse-shape discriminator (PSD). The electronics circuit consisted of a TOF circuit and the PSD circuit of NIM modules⁶⁾. The TOF, PSD and pulse-height data were collected event by event as three parameter list data with a magnetic-optical disk for off-line analysis.

To extend the measurable energy range of the secondary neutrons, we carried out two measurements for each angle, namely 1) high energy run and 2) low energy run. In high energy run, we employed a larger NE213 detector, 14 cm-diam x 10 cm-thick, coupled to a Hamamatsu R1250 photo-multiplier with a tube base specially designed for high energy neutrons⁶⁾ around 11 m from the target and set the detector bias at 4.0 or 3.5 MeV proton using $^{241}\text{Am-Be}$ and ^{22}Na sources. In the low energy run, we adopted a smaller NE213 detector,

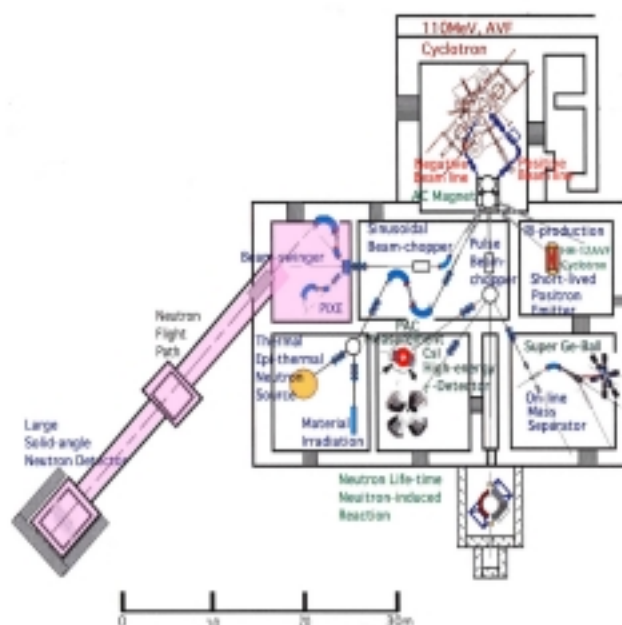


Fig.1: The layout of Tohoku University cyclotron beam transport system and experimental room. Accelerated beams are led to the target chamber attached to the beam swinger. The target room is connected to the neutron flight path.

5-cm-diam and 5-cm-thick, coupled to Hamamats R1828 photo-multiplier placed around 3.5 m from the target and biased around 0.6 MeV proton. The high energy run and low energy run covered the neutron energy range, 4.0 or 3.5 -70 MeV, and 0.6 – 30 MeV, respectively. The results by two runs were in good agreement in overlapping region. This technique enabled to obtain the data over almost entire energy range of secondary neutrons with good timing resolution for high energy region and a good signal-to-noise ratio for low energy region concurrently.

The pulse width was generally less than 1.0 ns in FWHM, and the overall timing resolution was 1.0-1.5 ns. The beam current on the target was 0.5-5 nA depending on the angle and run. The beam spot and position was adjusted and checked for each angle setting of beam swinger.

III. DATA ANALYSIS

In the data analysis, first, neutron TOF spectra were gated by the pulse-height bias and the PSD signal to select neutron events, and neutron TOF spectra for the pulse height bias were derived. Then, they were converted into the energy spectra according to the following relation between the neutron energy and TOF:

$$E_n(i) = mc^2 - m_0c^2 = m_0c^2 \left(1/\sqrt{1-\beta^2} - 1 \right), \quad \beta = v_n / c = L/(c \cdot T_n(i)),$$

where m_0 is the rest mass of a neutron, i is the channel number of the events, L is the flight path length and c is the light velocity. Then, the spectra were divided by the efficiency of the neutron detector, the solid angle and integrated charge to convert into differential yields per charge. The efficiency vs. energy curves for neutron detectors was obtained by the calculation using the Monte Carlo code SCINFUL⁷⁾ which verified to be accurate within $\pm 5\%$ up to 80 MeV by S. Meigo⁸⁾. In fact, response functions of the NE213 detectors derived from the pulse-height data during the measurement proved to agree well with the calculations. Neutron yields were normalized by the beam charge on the targets counted by the current digitizer, model ORTEC-439 except for the case of aluminum target which was slightly thinner than the proton range. In this case, the beam charge was interpolated from runs before and after the aluminum runs. This procedure provided reasonable results owing to the stable beam condition.

The operation of the beam chopping system eliminated almost completely the interference of the frame-overlap, and enabled to derive the neutron spectrum over wide energy range without difficulty.

The results obtained were corrected further for the effects of a) neutron attenuation within the target, b)neutron attenuation in the air and wall of target chamber. The corrections were done using the experimental neutron total cross-section data by Finlay et al⁹⁾. The correction for a) was largest for the measurements at 90-deg. because secondary neutrons transmit the target perpendicularly and amounted to around 30 % for Ta and W target. It should be pointed out that prior to the correction, the experimental data for low energy neutrons of Ta and W show significant forward rise but correction led to almost isotropic distributions. This result indicated the validity of the correction. The correction (b) was significant only for low energy neutrons less than a few MeV. Background events due to gamma-rays which could not be eliminated by PSD were rejected by subtracting flat component in the TOF spectrum from each channel.

The error of the experimental results were estimated by the quadratic sum of 1)statistical error, 2)detector efficiency, and 3)the data correction for neutron attenuation.

IV. RESULTS

IV-1 General

In the present study, data were obtained for neutron emission spectra for each emission angle. From the data, the angular distribution for each outgoing energy was derived too.

In the following, experimental results are presented. The (p,n) data are compared with the recent data library LA-150. Other experimental data which are directly comparable with the present results are very few. For the Li(d,n) reaction, similar experimental data by Lone et al for Ed=23 MeV and at 0-deg¹⁰⁾. are available and shown in Fig.2 together with the present results. Allowing for the difference in incident energy, the Lone et al's data are

in good agreement with the present ones in the energy region above ~ 5 MeV, which means the validity of the experiment and data analysis of the present experiment. However, in lower energy region, the data by Lone et al are much higher than the present one. For the following reasons, we believe that our data are more reasonable than the Lone et al's one. First, from the view point of kinematics, it is unlikely that so much amount of low energy neutrons are emitted to 0-deg from the (d,n) reaction on such a light element as lithium which shows a very strong effect of center-of-mass motion. Second, we paid attention on the determination of the detector bias and the efficiency in PSD. The PSD performance was excellent in particular for smaller NE213 detector and the PSD efficiency could be assumed to be $\sim 100\%$ even for low energy neutrons in question.

IV-2 C, Al, Ta, W (p,n) spectra

The thick target neutron yields from C, Al, Ta and W are shown through fig.3 to fig.8. For, C, Al and W, the data of LA-150 are also shown. For Ta, LA-150 data are not available.

First, it should be noted that the present data covers almost entire secondary energies and clearly show the mass and angular dependence of neutron spectrum. The neutron spectra vary drastically from carbon to tantalum and tungsten, and the angular dependence becomes forward peaking with increasing outgoing energy because of increasing contribution of non-equilibrium processes.

The spectrum of the C(p,n) reaction are much softer than others as expected. In this case, LA-150 data show marked difference from the present one in high energy region. One reason is the

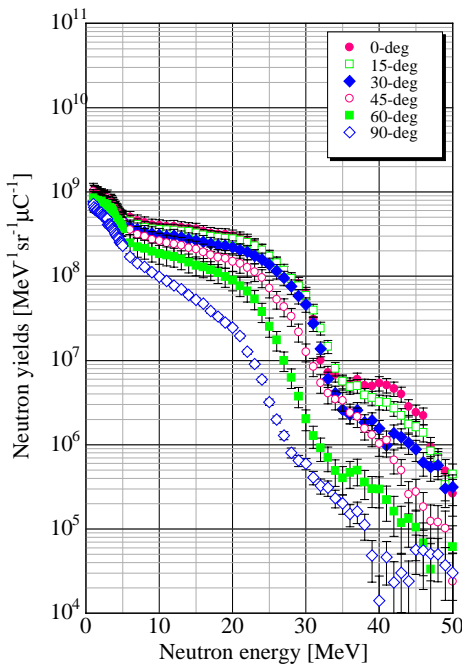


Fig.3: Energy spectra from thick target of ^{nat}C as a function of emission angle.

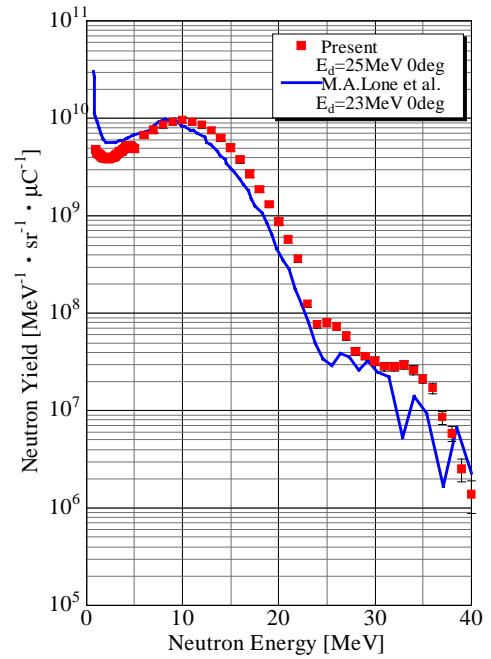


Fig.2; Comparison of the present results of $\text{Li}(d,n)$ spectrum at $E_d=25$ MeV with that by Lone et al., at $E_d=23$ MeV.

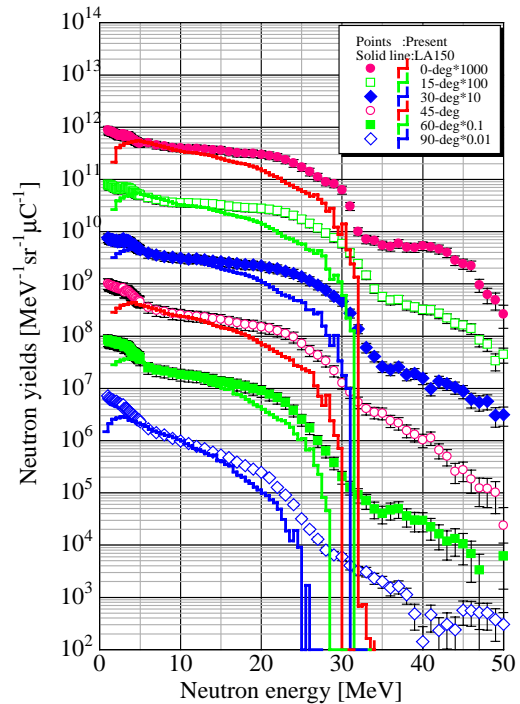


Fig.4: Comparison of the present results for ^{nat}C with the LA-150 data.

milder spectrum of the $^{12}\text{C}(p,n)$ neutrons and the other one is that LA-150 lacks the $^{13}\text{C}(p,n)$ component which extends to high energy because of much shallower Q-value (-3.0 MeV). These differences in neutron spectrum may lead to underestimation of neutrons transmitting or leaking from bulk shields. Therefore, in some cases, the ^{13}C contribution should be considered appropriately in neutron shielding designs.

The emission spectra of aluminum (Fig.5) are more continuous and extend to higher energy than in the carbon case because of shallower Q-value (-5.59 MeV) and the mono-isotopic nature. The LA-150 data show fairly good agreement with the present one except for the high energy ends in forward angles. It is apparent that the neutron yields of aluminum is smaller significantly than tantalum and tungsten while the spectrum is harder significantly.

The emission spectrum from tantalum and tungsten (Fig.6-Fig.8) is very similar both in the shape and the magnitude. Both spectra show large evaporation peaks and smaller contribution of high-energy neutrons which favors the application to a moderated neutron source. In both data, low energy neutrons show isotropic angle dependence while higher energy neutrons show marked forward rising. Previously there was an argument that the neutron yield of tungsten is larger than tantalum, but the present data indicated that the neutron yields are same for both within experimental uncertainty.

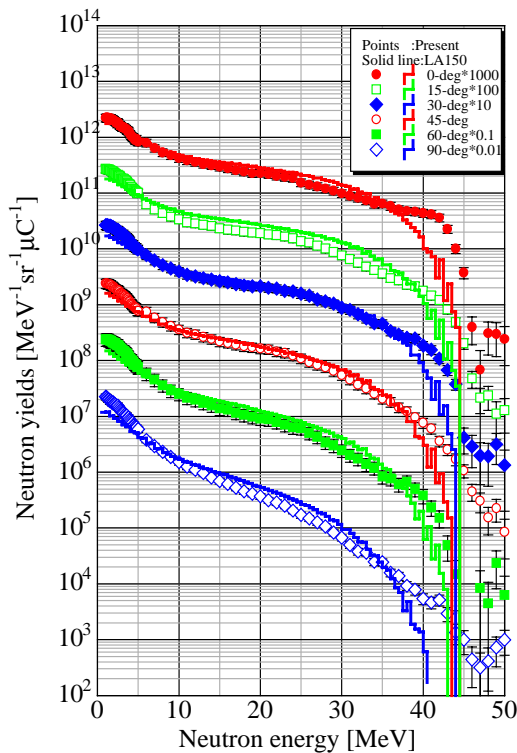


Fig.5: Neutron emission spectra of aluminum in comparison with LA-150.

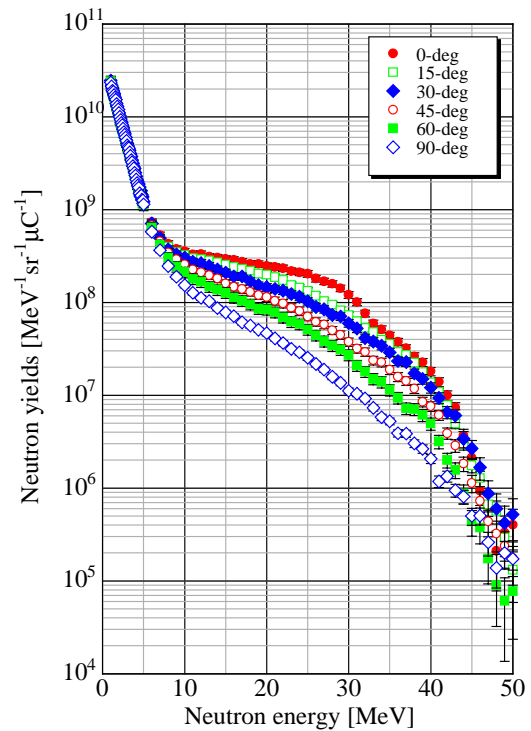


Fig.6: Angle dependence of neutron emission spectrum of tantalum.

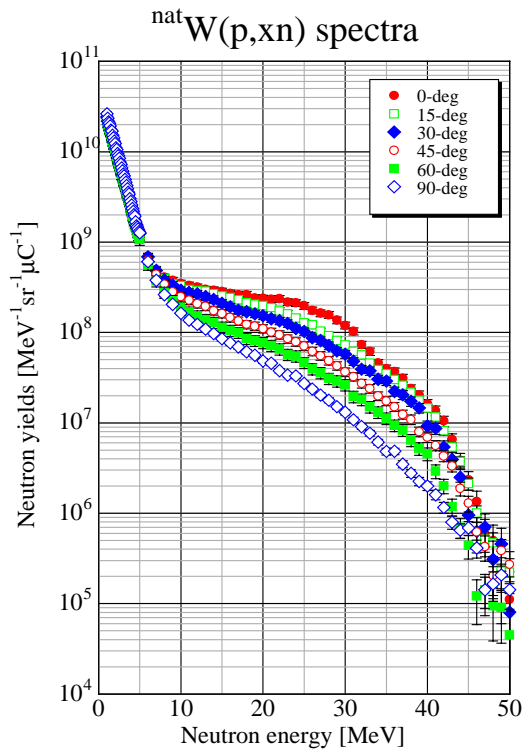


Fig.7: Angle-dependence of neutron emission spectra from thick target of tungsten.

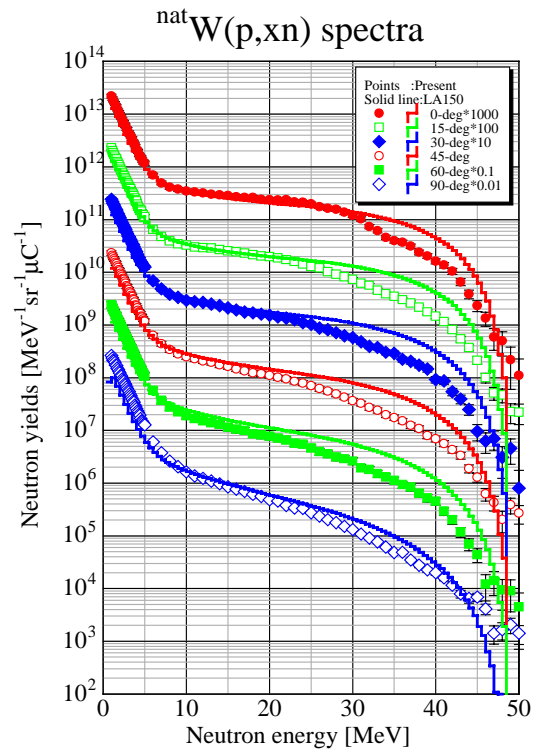


Fig.8: Neutron emission spectra of tungsten, compared with LA-150.

IV-3 Li(d,n) and Be(d,n) spectra

The neutron emission spectra from thick lithium and beryllium targets bombarded by 25 MeV deuterons are shown in Fig.9 and Fig.10. As noted in sect. IV.1, the present results for lithium is in good agreement with Lone et al's one above ~ 5 MeV.

The Li, Be(d,n) spectra have broad peaks around 10 MeV which are expected as intense neutron source to simulate high neutron flux environment in d-T fusion reactors. In the case of Li, however, the spectrum extends to higher energies up to 40 MeV due to large Q-values of the ${}^7\text{Li}(d,n)$ reaction (15.03 MeV). This so called "high energy tail" introduces problems in the shielding of the facility and the assessment of the radiation effects in the neutron irradiation field. The present results indicate that the broad peak around 10 MeV decrease monotonically with increasing angle, but the "high energy tail" peaks around 20-deg. not in 0-deg., which can be interpreted by the transferred angular momentum in the reaction.

In the case of Be, there is no high-energy tail because of smaller Q-value for ground state transition (4.36 MeV). It should be noted that for the case of Be too, the present data do show so much neutron yield than observed in the data of Lone et al¹⁰.

The neutron yields from the Li, Be(d,n) reactions are relatively high in forward direction. However, the neutron spectra are much harder than in the Ta, W(p,n) reaction. It may cause difficulty to obtain moderated neutron fields.

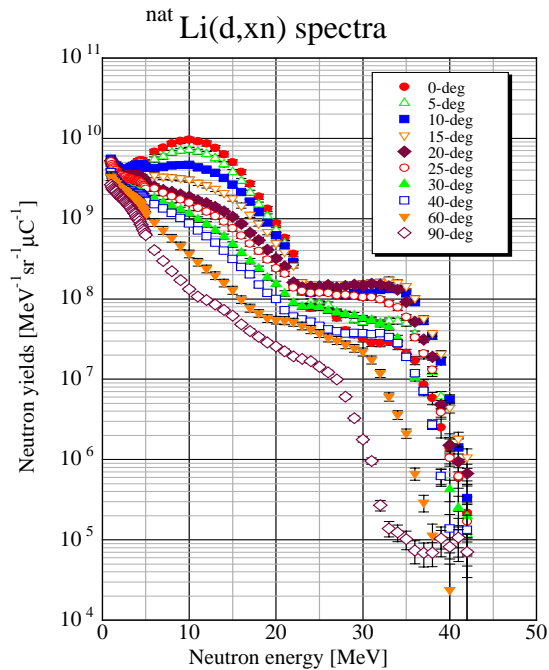


Fig.9: The neutron yields of the ${}^{\text{nat}}\text{Li}(d,n)$ reaction for incident deuteron energy of 25 MeV.

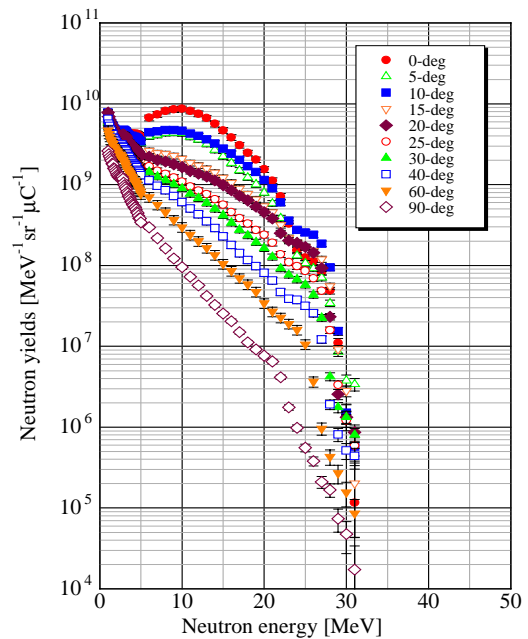


Fig.10: The neutron yields of the $\text{Be}(d,n)$ reaction for incident deuteron energy of 25 MeV.

V. SUMMARY

We have measured differential thick target neutron yields from the

- 1) C, Al, Ta, W (p,n) reactions for 50 MeV protons, and
- 2) Li, Be(d,n) reactions for 25 MeV deuterons,

which are of great importance for accelerator shielding and for optimization of neutron production targets.

The emission spectrum data were obtained successfully over almost entire range of secondary neutrons by carrying out two measurements optimizing the experimental conditions for the high energy and low energy region. The experimental data obtained demonstrated the dependence of neutron spectrum on target mass and emission angle which will be useful shielding design of accelerator system and for target design. The present (p,n) data indicated problems in the data file of LA-150 and will be useful for the improvement of the nuclear data evaluation code and method.

The experiments are being extended to other incident energies and targets. In the near future, these results will be presented.

REFERENCES

1. e.g., Intense proton Accelerator Project in Japan: http://jkj.tokai.jaeri.go.jp/index_j.html
2. IFMIF CDA TEAM, IFMIF Conceptual Design Activity Final Report edited by Marcello Martone, Report 96.11, Enea, Dipartimento Energia, Frascati (1996)
3. <http://www.cyric.tohoku.ac.jp>,
4. A.Terakawa et al.: Nucl. Instrum. Methods., in print
5. M. B. Cadwick et al., Nucl. Sci. Eng., 1331, (1999) 293
6. M. Baba et al., J. Nucl. Sci. Technol., Vol. 27., No.7, (1990) 601
7. J. K. Dickens, ORNL-6436, Oak Ridge National Laboratory, 1988
8. S. Meigo Nucl. Instrum. Methods in Physics Research A 401 (1997) 365
9. R.W Finlay et al.: Phys. Rev., C47 (1993) 239
10. M. A. Lone et al.: Nucl. Instrum. Methods, 141 (1977) 331